The Response of Liquid-Filled Pipes to Vapour Cavity Collapse

TIJSSELING A. S.
Delft University of Technology & Delft Hydraulics, Delft, The Netherlands
FAN D.
University of Dundee, Dundee, UK

ABSTRACT

The collapse of vapour cavities in liquid is usually accompanied with almost instantaneous pressure rises. These pressure rises impose severe loads on liquid-conveying pipes whenever the cavities become sufficiently large. Due to the impact nature of loadings, movement of the pipe walls can be expected.

Tests are performed in a water-filled closed pipe suspended by thin steel wires. Vaporous cavities are induced in the liquid by hitting the pipe axially by a steel rod. The volume of the cavities can be varied by changing the initial pressure of the water. The developing and collapsing of cavities in the liquid is inferred from pressure measurements. Strain gauges and a laser Doppler vibrometer are used to record the response of the pipe to these pressures.

The test results are compared with predictions from a numerical model. The model describes 1) axial stress wave propagations in the pipe and 2) water hammer and cavitation phenomena in the liquid. Pipe and liquid interact via 1) the radial expansion and contraction of the pipe wall and 2) the closed ends of the pipe, where large vapour cavities may develop.

1 INTRODUCTION

Pipe systems experience severe dynamic loads when they are subjected to water hammer. Particularly in the case that water hammer is accompanied with cavitation, pressure waves with steep fronts may occur due to the collapse of large vapour bubbles or column separations. Under such circumstances the pipe system, which is never entirely rigid, will move. This movement introduces new pressure waves in the fluid, so that an interaction exists between the transient behaviour of pipe system and fluid.

Vardy and Fan (1989) investigated fluid-structure interaction phenomena in a straight elastic pipe. They considered, beside pressure waves in the fluid, both axial and flexural stress waves in the pipe wall. Excellent agreement was found between theory and experiment. Cavitation was not part of Vardy and Fan's work.

However, the experimental apparatus they set up is also found to be suitable for cavitation tests. The authors performed these tests for axial pipe motions. Part of the results is presented in this paper. The experimental results are compared with predictions from a mathematical model. This enables the authors to validate the model and simultaneously gives them a better understanding of the physical phenomena involved.

SMiRT 11 Transactions Vol. J (August 1991) Tokyo, Japan, © 1991

2 EXPERIMENT

The principal part of the experimental apparatus is a 4.5 m long stainless steel pipe with an outer diameter of 59.9 mm and a wall thickness of 3.9 mm. The pipe is closed at both ends and filled with pressurized tap water. It is suspended by two long steel wires so that it can move freely in the horizontal plane. Axial stress waves in the pipe wall and pressure waves in the water are generated simultaneously by the external impact of a solid steel rod onto one of the pipe's ends. See figure 1.

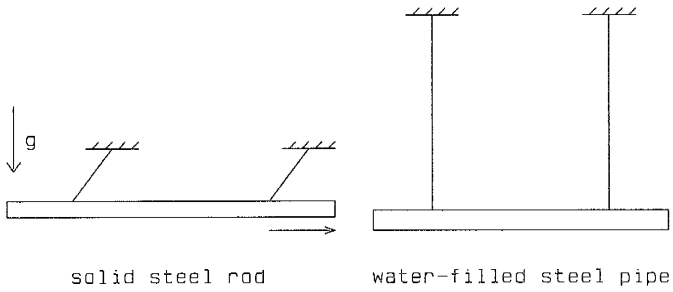

Fig. 1 Schematic of experimental apparatus

Vardy and Fan (1989) prevented the occurrence of cavitation by taking the initial pressure of the water high enough in relation to the impact velocity of the rod. In the present study the initial pressure of the water is deliberately lowered, so that cavitation will occur. The magnitude of the initial pressure defines the severity of cavitation. Severe cavitation takes place when the initial pressure is atmospheric. There is no cavitation when the initial pressure is higher than 1.8 MPa. This limit value depends on the impact velocity of the rod, which was measured 0.739 m/s for the results presented herein.

The amount of free gas in the water is expected to be negligible, since the water is pressurized. Gas release during transient events does not play a role, as a consequence of the time scale of the tests (milliseconds). For the same reason friction can be disregarded. Hence, the experiment isolates vaporous cavitation in combination with fluid-structure interaction.

The pipe is extensively instrumented with strain gauges and pressure transducers. A laser Doppler vibrometer is used to measure the velocity of the pipe wall. It was also used to measure the impact velocity of the rod. In the cavitation tests axial strains were measured at four locations at the top of the pipe. Pressures were measured in the middle of the remote end cap and at four locations along the bottom of the pipe. The velocity of the pipe wall was measured close to the impact end.

3 CALCULATION

Calculations are carried out with a one-dimensional model simulating the acoustic behaviour of thin-walled, elastic, liquid-filled pipes. Fluid-structure interaction and cavitation phenomena are taken into account. The model is partly described in (Tijsseling and Lavooij 1989). It is a combination of 1) the four-equation model for axial fluid-structure interaction problems (Schwarz 1978, Wiggert et al. 1985) and 2) the concentrated cavity model for cavitation due to water hammer (Provoost, 1976). The underlying basic equations are:

$$\frac{\partial \dot{u}_z}{\partial t} - \frac{1}{\rho_t} \frac{\partial \sigma_z}{\partial z} = 0 \qquad (1)$$

$$\frac{\partial \dot{u}_z}{\partial z} - \frac{1}{\rho_t c_T^2} \frac{\partial \sigma_z}{\partial t} = - \frac{\nu}{E} \frac{R}{e} \frac{\partial P}{\partial t} \qquad (2)$$

$$\frac{\partial V}{\partial t} + \frac{1}{\rho_f} \frac{\partial P}{\partial z} = 0 \qquad (3)$$

$$\frac{\partial V}{\partial z} + \frac{1}{\rho_f c_F^2} \frac{\partial P}{\partial t} = 2\nu \frac{\partial \dot{u}_z}{\partial t} \qquad (4)$$

in which:
- c_F = pressure wave speed
- c_T = axial stress wave speed
- E = Young's modulus
- e = pipe wall thickness
- P = fluid pressure
- R = internal radius of pipe
- t = time
- $\dot{u}_z$ = axial velocity of pipe
- V = fluid velocity
- z = distance along the pipe
- ν = Poisson's ratio
- ρ_f = fluid density
- ρ_t = density of pipe wall
- σ_z = axial pipe stress

The pipe equations (1) and (2) describe the propagation of axial stress waves in the pipe wall, the liquid equations (3) and (4) are extended water hammer equations. Terms due to friction and gravitation are left out. The pipe and liquid equations are coupled via the right-hand sides, representing the expansion and contraction of the pipe wall. Due to this coupling, the theoretical wave speeds c_t and c_f slightly differ from the classical values defined by:

$$c_T = \{\frac{E}{\rho_t}\}^{\frac{1}{2}} \quad \text{and} \quad c_F = \{\frac{\rho_f}{K_f} + 2\rho_f \frac{R}{e} \frac{(1-\nu^2)}{E}\}^{-\frac{1}{2}} \qquad (5)$$

in which K_f is the bulk modulus of the liquid. The pipe and liquid equations are also coupled via boundary conditions. In the experiment this coupling is caused by the mutual forces existing between cap and liquid at the pipe's ends. The axial stress σ_z and the hoop stress σ_ϕ are related to the axial strain ε_z and the pressure P, quantities that are measured in the experiment, by:

$$\sigma_z = \nu \frac{R}{e} P + E \varepsilon_z \quad \text{and} \quad \sigma_\phi = \frac{R}{e} P \qquad (6)$$

Equations (1)-(4) are solved simultaneously by the method of characteristics, for given initial and boundary conditions. Solutions were calculated every 0.11 ms at 151 equidistant locations along the pipe. The end caps are modelled as lumped masses, the influence of their inertia is not negligible. Details of the numerical method, in which vapour cavities are allowed to form at the pipe's ends, can be found in (Tijsseling and Lavooij 1989). Here, however, cavities are allowed to form not only at the pipe's ends, but also at 149 locations along the pipe. Whenever at some location the pressure drops to the vapour pressure, which is the bottom level in the model, a cavity is assumed to form. The volume V of the cavity follows from a mass balance:

$$\frac{dV}{dt} = -A_f (V_1 - V_2) \qquad (7)$$

where A_f is the cross-sectional discharge area, and V_1 and V_2 stand for the fluid velocities at either side of the cavity. The cavity disappears when its volume is calculated to be less than zero. At room temperature the vapour pressure is about 0.002 MPa.

4 RESULTS

Experimental and theoretical results for three levels of cavitation are presented in figure 2. The three levels, classified as slight, moderate and severe, correspond to initial water pressures 1.07 MPa, 0.70 MPa and 0.18 MPa respectively. The no cavitation results with initial pressure 2 MPa are given for comparison.

Figure 2 consists of four sets of five graphs. The upper and lower graphs in each set depict the volumes of the vapour cavities at the pipe ends, as calculated by the model. Note that the scale of the upper graph (volume at impact end) is ten times smaller than the scale of the lower graph (volume at remote end). The central three graphs show measured and calculated time histories of 1) the velocity of the pipe wall near the impact end, 2) the axial strain 1.69 m away from the impact end, and 3) the pressure in the middle of the pipe.

The overall agreement between experiment and calculation is good. In particular, the model predicts with great accuracy the beginning of the events. This justifies the use of the model in explaining some aspects of the experiment.

The impact of the rod generates an axial compression wave in both pipe wall and liquid. The stress wave in the pipe wall dominates the beginning of the events, since it travels more than four times as fast as the pressure wave in the liquid. After passage of the stress wave, the axial velocity of the pipe is 0.55 m/s and the liquid pressure dropped 0.14 MPa due to the radial expansion of the pipe wall. These effects are observed in all four cases. After approximately 1 ms the compression wave reaches the remote end, thereby pushing the end cap away from the liquid. Due to the inertia of the liquid, a cavity develops for those cases where the initial pressure in the pipe is low. From the calculated volumes it is seen that the largest cavity forms now. When the reflected stress wave reaches the impact end again, pipe and rod separate. The pipe velocity increases a second time, to values between 0.75 m/s and 0.94 m/s, depending on the amount of cavitation.

The axial strains, shown in the middle graphs, attain extreme values during the contact time of pipe and rod. After this time the pipe has two free ends, which results in dynamic strains oscillating around the zero level. The response to the rod impact is different in all four cases. Any response to the collapse of the calculated large cavity is not discernible.

5 CONCLUSIONS

Experimental and theoretical results are obtained for the response of a liquid-filled pipe to axial impact. Emphasis is placed on the formation of vapour cavities in the liquid. In the presented experiment the collapse of cavities did not lead to extreme pipe responses. The developed mathematical model gives reliable results for all levels of cavitation.

REFERENCES

Provoost, G.A. (1976). Investigation into cavitation in a prototype pipeline caused by water hammer. Proc. 2nd Int. Conf. on Pressure Surges, BHRA, London, UK, September 1976, pp. 13-29.

Schwarz, W. (1978). Druckstossberechnung unter Berücksichtigung der Radial- und Längsverschiebungen der Rohrwandung. Universität Stuttgart, Institut für Wasserbau, Mitteilungsheft 43. (In German).

Tijsseling, A.S. and Lavooij, C.S.W. (1989). Fluid-structure interaction and column separation in a straight elastic pipe. Proc. 6th Int. Conf. on Pressure Surges, BHRA, Cambridge, UK, October 1989, pp. 27-41.

Vardy, A.E. and Fan, D. (1989). Flexural waves in a closed tube. Proc. 6th Int. Conf. on Pressure Surges, BHRA, Cambridge, UK, Oct. 1989, pp. 43-57.

Wiggert, D.C., Otwell, R.S. and Hatfield, F.J. (1985). The effect of elbow restraint on pressure transients. Journal of Fluids Engineering, ASME, Vol. 107, No. 3, pp. 402-406.

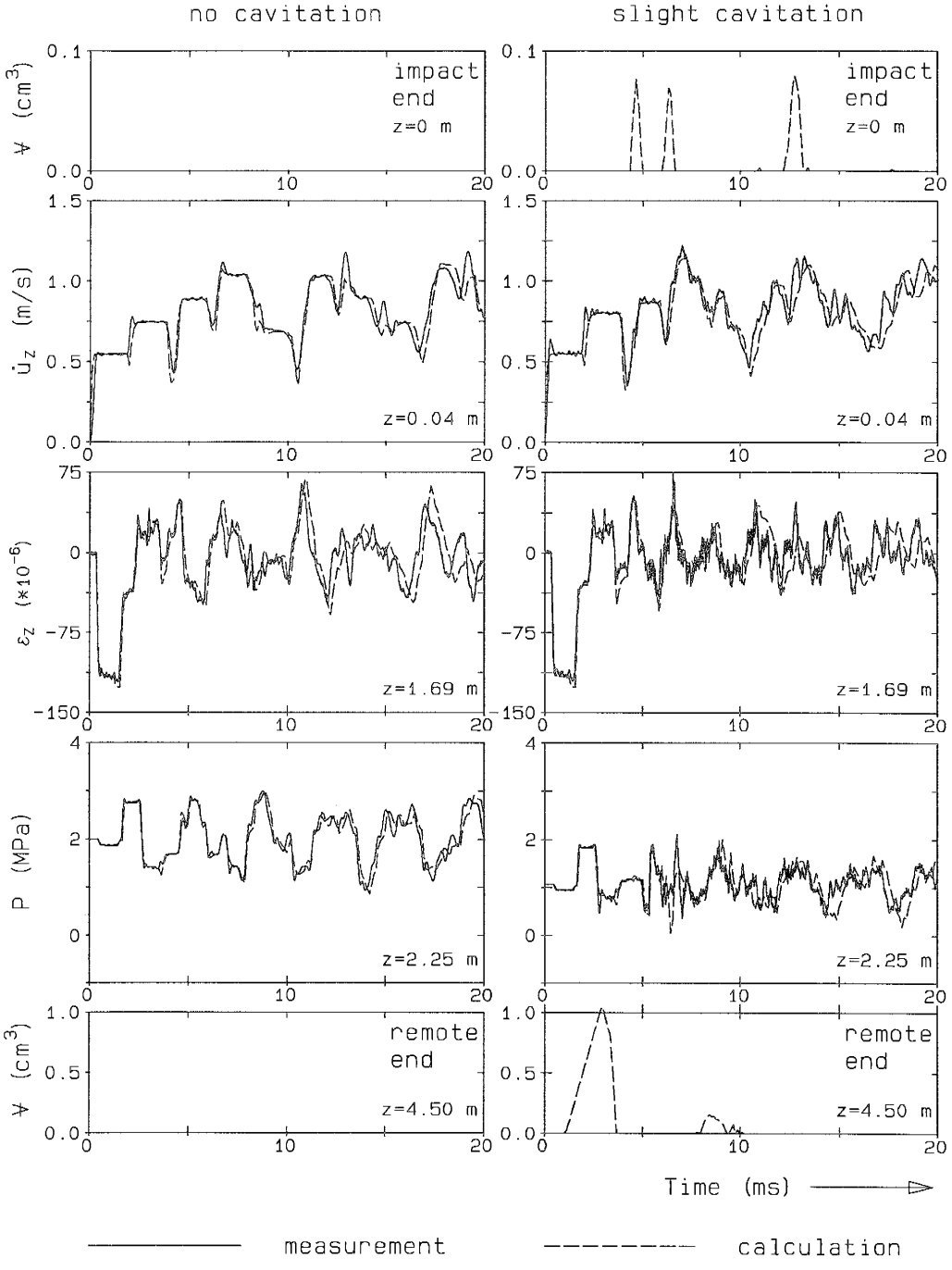

Fig. 2 Experimental and theoretical results

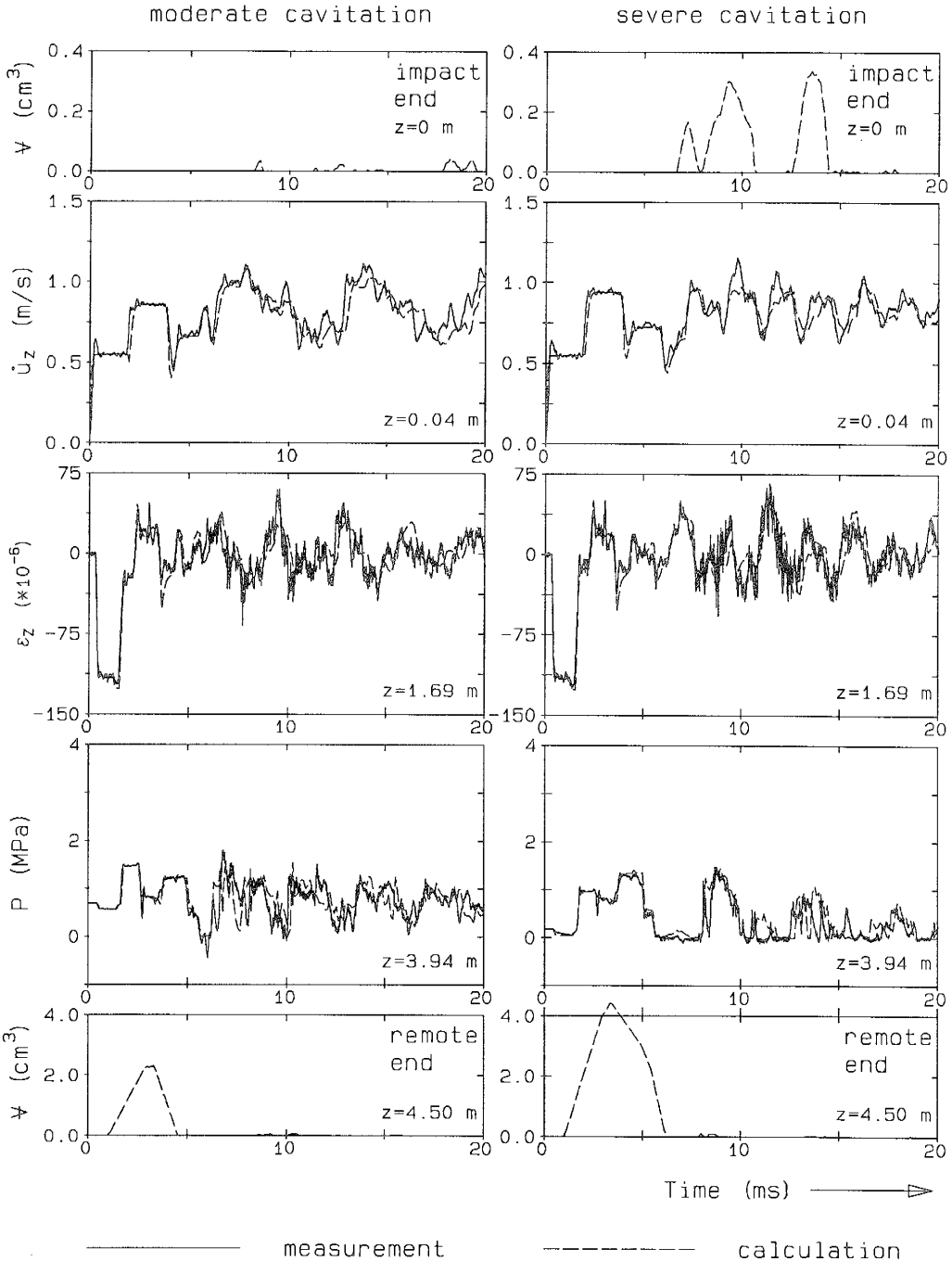

Fig. 2 (continued)